

β 3: An additional auxiliary subunit of the voltage-sensitive sodium channel that modulates channel gating with distinct kinetics

Kevin Morgan*, Edward B. Stevens†, Bhaval Shah†, Peter J. Cox‡, Alistair K. Dixon†, Kevin Lee†, Robert D. Pinnock†, John Hughes†, Peter J. Richardson‡, Kenji Mizuguchi*, and Antony P. Jackson*[§]

Departments of *Biochemistry, and †Pharmacology, University of Cambridge, Tennis Court Road, Cambridge, United Kingdom CB2 1QW; ‡Parke-Davis Neuroscience Research Centre, Cambridge University Forvie Site, Robinson Way, Cambridge, United Kingdom CB2 2QW

Edited by William A. Catterall, University of Washington School of Medicine, Seattle, WA, and approved December 15, 1999 (received for review August 24, 1999)

The voltage-sensitive sodium channel confers electrical excitability on neurons, a fundamental property required for higher processes including cognition. The ion-conducting α -subunit of the channel is regulated by two known auxiliary subunits, β 1 and β 2. We have identified rat and human forms of an additional subunit, β 3. It is most closely related to β 1 and is the product of a separate gene localized to human chromosome 11q23.3. When expressed in *Xenopus* oocytes, β 3 inactivates sodium channel opening more slowly than β 1 does. Structural modeling has identified an amino acid residue in the putative α -subunit binding site of β 3 that may play a role in this difference. The expression of β 3 within the central nervous system differs significantly from β 1. Our results strongly suggest that β 3 performs a distinct neurophysiological function.

The voltage-sensitive sodium channel plays a fundamental role in excitable cells, transiently increasing the sodium permeability of the plasma membrane in response to changes in membrane potential and thus propagating the action potential (1, 2). Not surprisingly, mutations in sodium channel genes are implicated in several pathologies, including epilepsy and cardiac arrhythmias (3–5), and therapeutic drugs, including antiepileptics, local anesthetics, and anticonvulsants (6), act on the channel.

In the central nervous system, the channel is conventionally described as a heterotrimer composed of a 260-kDa α -subunit, a noncovalently associated 36-kDa β 1-subunit, and a disulfide-linked 33-kDa β 2-subunit (2). The α -subunit forms the ion pore and is responsible for the voltage-sensitive characteristics of the complex. There are multiple isoforms of the α -subunit expressed in different regions of the brain and peripheral nervous system that differ in their kinetic properties (1). The β -subunits are auxiliary components acting in a regulatory capacity (7). β 1 increases the fraction of α -subunits operating in a fast gating mode, thus accelerating the activation and inactivation kinetics of the channel and modulating the frequency with which neurons fire (8). The β 2-subunit is required for the efficient assembly of the channel but has minor effects on gating kinetics. These two β -subunits are distantly related by sequence (9).

We now report the cloning and analysis of the rat and human forms of a previously uncharacterized sequence that we call β 3. It is homologous to β 1, but differs from β 1 both in its distribution within the brain and in some of its kinetic properties. The discovery of this subunit increases the complexity of the sodium channel and raises further questions about the role of these auxiliary subunits.

Materials and Methods

Cloning Methodology. We isolated a variant of the rat pheochromocytoma cell line PC12 (termed A35C), which lacks typical neuronal properties (10). To discover previously unidentified neuroendocrine-specific genes, subtractive cloning was used to identify transcripts expressed at a level in the variant cells lower than that in normal PC12 cells. Total RNA was prepared from the PC12 cells, and the A35C variant and poly(A)⁺ RNA were purified by oligo(dT) cellulose column chromatography (11). Subtractive cloning was carried out by using the technique of PCR selection (12).

Amplified cDNA fragments derived from genes differentially expressed in normal PC12 cells were subcloned into a cDNA fragment library (11). Plasmid minipreps from randomly picked subclones were sequenced (Department of Biochemistry, University of Cambridge) and screened through DNA database searches. Full-length coding sequence for rat β 3 was isolated by screening a rat brain cDNA library in the vector λ Zap (Stratagene) with a ³²P-labeled partial β 3 clone. A human β 3 cDNA clone was isolated from a human striatal library in λ Zap II (Stratagene) screened with ³²P-labeled full-length rat clone. Both cDNA strands were sequenced with M13 and internal primers.

Chromosomal Location. Radiation hybrid mapping (13) was used to identify the chromosomal location of the human β 3 gene. PCR primers were designed against the 3' untranslated sequence of human β 3. Forward primer: 5'-GTCCAGTGGGGTCGCTTAG-3'. Reverse primer: 5'-CAGAGAGATTCCCTCGGTCA-3'. PCR was performed in 20 μ l of 45 mM Tris-HCl, pH 8.1/12.5% (wt/vol) sucrose/12 mM (NH₄)₂SO₄/3.5 mM MgCl₂/0.5 mM dNTPs/0.6 unit of AmpliTaq (Perkin-Elmer) with 100 ng of the forward and reverse primer for 35 cycles. The cycling conditions were 92°C (denaturation for 0.5 min), 55°C (annealing for 1 min), and 72°C (extension for 1 min). The primers were used to screen the GeneBridge 4 radiation hybrid panel, which consists of 93 human-hamster somatic cell lines (Research Genetics, Huntsville, AL). Under the PCR conditions used, a single band was amplified from human genomic DNA but not from hamster genomic DNA. The PCRs were repeated in three separate experiments to confirm reproducibility. Each cell line in the collection was individually scored 1 for the presence or 0 for the absence of the appropriate PCR band (ambiguous results were scored 2). The complete scores for all cell lines were assembled in a defined order (the data vector) and submitted to the Whitehead/MIT Center for Genome Research Database (<http://www-genome.wi.mit.edu/cgi-bin/contig/rhmapper.pl>) for comparison with a panel of standard sequenced tagged site markers whose chromosomal locations had already been established.

Northern Blotting. Approximately 10 μ g of total RNA was extracted from adult rat tissues and PC12 cells, denatured in 50% (vol/vol) formamide/6% (vol/vol) formaldehyde/1 \times Mops [pH 7.0; 3-(N-morpholino)propanesulfonic acid] at 65°C for 5 min, and separated by electrophoresis through 1% agarose gel containing 6% (vol/vol) formaldehyde/1 \times Mops (pH 7.0). Samples were transferred to

This paper was submitted directly (Track II) to the PNAS office.

Abbreviation: kb, kilobase.

Data deposition: The sequences reported in this paper have been deposited in the EMBL database (accession nos. AJ243395 and AJ243396).

[§]To whom reprint requests should be addressed. E-mail: a.p.jackson@bioc.cam.ac.uk.

The publication costs of this article were defrayed in part by page charge payment. This article must therefore be hereby marked "advertisement" in accordance with 18 U.S.C. §1734 solely to indicate this fact.

Article published online before print: *Proc. Natl. Acad. Sci. USA*, 10.1073/pnas.030362197. Article and publication date are at www.pnas.org/cgi/doi/10.1073/pnas.030362197

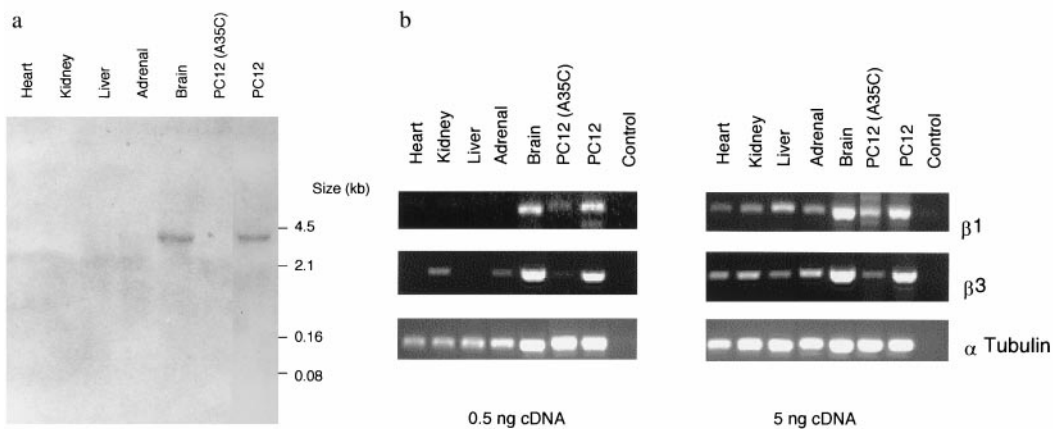


Fig. 1. $\beta 3$ expression in cells and tissues. (a) Northern blot of $\beta 3$ expression in rat tissues and PC12 cell lines. (b) Expression of $\beta 3$ and $\beta 1$ in rat tissues, PC12, and A35C variant cell lines detected by PCR at each of two cDNA concentrations.

Hybond N membrane and prehybridized at 55°C in 6× SSC/2× Denhardt's solution/0.1% SDS/50 μg/ml denatured herring sperm DNA. Blots were hybridized overnight at 55°C in fresh buffer containing 5 × 10⁶ cpm ³²P-labeled 2.2-kilobase (kb) rat $\beta 3$ cDNA probe (specific activity 10⁸ cpm/μg). The membrane was washed once in 2× SSC/0.1% SDS at 65°C for 30 min and twice in 0.1× SSC/0.1% SDS at 65°C for 30 min each (11).

Tissue Expression by PCR. Total RNA was prepared from adult rat tissues and PC12 cells, treated with DNase I to remove genomic contamination, and reverse transcribed with Moloney murine leukemia virus reverse transcriptase with anchored oligo(dT) primer according to the manufacturer's recommendations. Approximately 0.5 and 5 ng of cDNA was separately subjected to PCR amplification by using primers specific for rat $\beta 1$ (EMBL accession no. m91808), rat $\beta 3$ (AJ243395), and to ensure that similar amounts of cDNA were used in each reaction, rat α -tubulin (V01226). The primers used were chosen to correspond to unique sequences in the 3' untranslated region of each β -subunit: $\beta 1$ forward primer (nucleotides 1,103–1,120) 5'-GGTGAAGCAATATGGCCG-3'; reverse primer (nucleotides 1,317–1,300) 5'-AGATGAGGCCCA-GAACCC-3'; $\beta 3$ forward primer (nucleotides 1,942–1,961) 5'-GGAAGCTGACTGCCACAGAT-3'; reverse primer (nucleotides 2,209–2,190) 5'-CCTGGGGGACTTTACAAACA-3'; α -tubulin forward primer (nucleotides 298–316) 5'-CACTGGTACGTGGGTGAGG-3'; and reverse primer (nucleotides 469–448) 5'-

TTTGACATGATACAGGGACTGC-3'. PCR was performed as described above except that amplification reactions included 0.125 μl of Taqstart antibody (CLONTECH). A control amplification lacking cDNA was also included. After amplification, the products were separated on 2.5% agarose gels and visualized with ethidium bromide.

In Situ Hybridization. Whole brains were excised from adult (150- to 200-g) Wistar rats and snap frozen on dry ice. Cryostat (10-μm) sections were thaw mounted onto poly-L-lysine-coated slides, fixed with 4% (vol/vol) paraformaldehyde in PBS (pH 7.4), dehydrated, and stored under ethanol until hybridization. The sequence and location of the antisense oligonucleotides used for analysis were as follows: rat $\beta 1$ (nucleotides 1,296–1,252) 5'-GCTTGATGGGGT-GAAGAGGGGTCCGGACAGGGACAGTAGTGGGC-3'; rat $\beta 3$ (nucleotides 389–345) 5'-GGGAAGCAATCTGTTGAAG-GCAGGCATCTTTCCACCGTAAGCG-3'; and rat α IIA (nucleotides 1,659–1,615) 5'-GCAGAAATCCAGAGACT-TCAGCGGGGACAGCGGGATAGGTGTTTC-3'.

Oligonucleotides were 3' end-labeled with [³⁵S]dATP (Amersham Pharmacia; 1,000 Ci/mmol) by terminal deoxynucleotidyl transferase (Roche Molecular Biochemicals; ref. 11) and used for hybridization at a concentration of 400,000 cpm/100 μl of hybridization buffer. To confirm the specificity of the hybridizations, 100-fold excess of unlabeled oligonucleotide was added to the hybridization buffer in addition to the radiolabeled probe. Slides were air dried and hybridized overnight at 42°C in 150 μl of buffer containing 50% (vol/vol) formamide, 10% (vol/vol) dextran sulfate, 50 mM DTT, 1× Denhardt's solution, 0.5 mg/ml denatured salmon sperm DNA, and 0.5 mg/ml polyadenylic acid (all from Sigma). Sections were washed in 1× SSC at 55°C for 30 min, rinsed in 1× SSC, dehydrated, and apposed to Kodak Biomax MR x-ray film (Amersham Pharmacia) for 10 days. For cellular resolution, selected slides were subsequently dipped in photographic emulsion LM-1 (Amersham Pharmacia), incubated for 4 weeks, developed, and counter stained with Cresyl Violet.

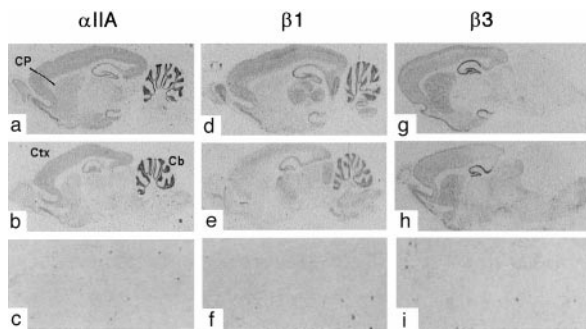


Fig. 2. *In situ* distribution of sodium channel subunits in adult rat brain. X-ray autoradiographs of separate sagittal sections of rat brain (taken from the same animal) showing the distribution of rat α IIA (a–c), rat $\beta 1$ (d–f), and rat $\beta 3$ (g–i) mRNA transcripts as revealed by *in situ* hybridization with specific oligonucleotide probes. Control reactions with 100-fold excess unlabeled probes are shown for α IIA (e), $\beta 1$ (f), and $\beta 3$ (i). Slides were exposed to x-ray film for 10 days. Dark areas indicate high expression levels. Cb, cerebellum; Ctx, cortex; CP, caudate putamen.

Electrophysiological Studies. Capped cRNAs for rat brain α IIA-subunit and rat $\beta 1$ - or $\beta 3$ -subunits were transcribed *in vitro* from linearized cDNAs (Promega). *Xenopus laevis* were anesthetized by immersion in 0.3% (wt/vol) 3-aminobenzoic acid (Sigma), and ovarian lobes were removed. Oocytes were dissociated by using 0.3% (wt/vol) collagenase (Sigma) in Ca²⁺-free solution (82.5 mM NaCl/2.5 mM KCl/1 mM MgCl₂/5 mM Hepes, pH 7.6). Prepared oocytes were microinjected with 50 nl of cRNAs dissolved in water. The cRNA concentration was estimated by UV spectrophotometry and agarose gel electrophoresis. Oocytes were incubated at 18°C in ND96 (96 mM NaCl/2 mM KCl/1.8 mM CaCl₂/1 mM MgCl₂/5 mM Hepes, pH 7.6). Two-electrode voltage clamp recordings were

Table 1. Detailed distribution of sodium channel subunits in the adult rat brain

Brain region	ROD		
	α IIA	β 1	β 3
Olfactory system			
Anterior olfactory	+++	1/2	+++
Olfactory tubercle	+++	1/2	+++
Piriform cortex	++++++	++	+++++
Neocortex			
Layer 2	+++	+	+++
Layer 3	+++	+	+++
Layer 4/5	++	+++	1/2
Layer 6a/6b	+++	0	+
Subiculum	++	1/2	++
Hippocampus			
CA1	++++	+++	++++++
CA2	++++++	+++	++++++
CA3	++++++	+++++	++++++
Dentate gyrus	+++++	+++	++++++
Hilus dentate gyrus	++	+	++
Indusium gresium	+++++	0	+
Tenia tecta	++++	+	++++++
Basal ganglia			
Caudate putamen	+	0	+++
Globus pallidus	0	0	0
Nucleus accumbens	+	0	++
VBD	1/2	0	1/2
Habenula	+++++	0	+++++
Amygdala	+	0	++
Hypothalamus	1/2	0	1/2
Preoptic area	1/2	0	1/2
Supraoptic	+	0	1/2
Mammillary body	+	0	+
Substantia nigra	1/2	0	1/2
VTA		+	0
Cerebellum			
Granular cell layer	++++++	+++++	0
Purkinje cell layer	+++	+++++	0
Molecular cell layer	0	0	0
Thalamus			
Reticular nucleus	0	1/2	0
Medial geniculate nuclei	1/2	++	0
Ventrolateral geniculate	++	+	1/2
Dorsal lateral nuclei	0	+	0
Anteroventral/dorsal nuclei	++	++	0
Ventral nuclei	+	1/2	0
Venteropostero nuclei	0	+	0
Midbrain			
Superior colliculus	1/2	0	1/2
APTd	++	1/2	1/2
DpMe	1/2	0	0
Oculomotor nucleus	+	0	1/2
Red nucleus	+	1/2	0
Interpeduncular nucleus	+	0	0
Inferior colliculus		1/2	1/2
Central grey		0	1/2
Brainstem			
Pontine nucleus	0	+++	0
Trapezoid body	+	++	0
Inferior olivary nucleus	0	+	1/2
Locus ceruleus	+	0	+
Raphe nuclei	0	1/2	0
Pontine reticular formation	0	1/2	0
Motor trigeminal nucleus	1/2	+	0
Me5 cells	+	0	0
Facial nuclei	0	1/2	0

Table 1. (continued)

Brain region	ROD		
	α IIA	β 1	β 3
Vestibular nuclei	0	1/2	0
Solitary nucleus	0	1/2	0
Cuneate nucleus	0	+++	0
Dorsal tegmental nucleus	+	1/2	+
Lateral parabrachial nucleus	+	0	0
Hypoglossal nucleus	1/2	0	0
Spinal trigeminal nucleus	1/2	1/2	0
Septum			
Bed nucleus stria terminalis	+	0	+
Lateral septal nucleus	+	0	+

In situ hybridization signal observed for ³⁵S-labeled oligonucleotide probes to rat α IIA, β 1, and β 3 mRNA on adult rat brain sections (emulsion-dipped sections and autoradiographs) were rated for relative optical density (ROD): ++++++, +++++, very abundant; +++++, abundant; +++, moderate; ++, +, low; 1/2, just above background; 0, not detectable ($n = 3-6$). VBD, nucleus of the vertical limb of the diagonal band; VTA, ventral tegmental area; APTD, anterior pretectal nucleus (dorsal part); DpMe, deep nucleus.

performed 3–6 days after microinjection of cRNAs by using a GeneClamp 500 amplifier (Axon Instruments, Foster City, CA) interfaced to a Digidata 1200 A/D board with CLAMPEX software (version 6, Axon Instruments). Oocytes were continually perfused with ND96. Microelectrodes filled with 3 M KCl had resistances between 0.5 and 2 M Ω . Currents were sampled at 10 kHz and filtered at 2 kHz. Data were analyzed with CLAMPFIT (version 6, Axon Instruments) and ORIGIN (version 5, Microcal Software, Northampton, MA). Exponential functions were fitted to data by using the simplex fitting algorithm in CLAMPFIT.

Results

Isolation and Chromosomal Location of β 3. Among the cDNA fragments isolated from the subtractive cloning was a 0.5-kb sequence encoding part of β 3. This sequence was used to screen a rat brain cDNA library from which a 2.2-kb cDNA clone containing the complete ORF was isolated. The human β 3 cDNA was subsequently identified by screening a human brain cDNA library with the 2.2-kb rat clone. The coding region of rat β 3 nucleotide sequence is 57% identical to rat β 1 and 40% identical to rat β 2. It is a separate gene product.

The data vector obtained for human β 3 from PCR amplification of the GeneBridge 4 panel of human-hamster hybrid cell lines was 1010110011 1000011100 0100010010 0000000000 0000111101 1120110000 0000100010 0001100001 1100001000 001. Statistical analysis indicated that the β 3 locus mapped to chromosome 11. The optimum position was 1.61 centiRays from sequenced tagged site marker D11S936 (logarithm of odds score = 2.05 relative to the next best placement). This sequenced tagged site marker has previously been mapped to 11q23.3 (<http://www-iaq.unice.fr/workshop>).

β 3 Expression. A ³²P-labeled cDNA probe corresponding to the full-length coding sequence of β 3 detected a single band of 4 kb on a Northern blot of rat brain and PC12 cells (Fig. 1a). This band is significantly larger than expected from the estimated molecular mass of the protein and presumably reflects a long 5' and/or 3' untranslated sequence. Under the high-stringency hybridization and washing conditions used, we did not observe crossreactivity with the 1.4-kb band characteristic of β 1 mRNA (8). To detect lower levels of β 3 expression and to compare them with β 1, we used the more sensitive technique of reverse transcription and PCR. A single amplification band of the expected size (148 bp for β 1 and 197 bp for β 3) was observed but was not present in the absence of cDNA

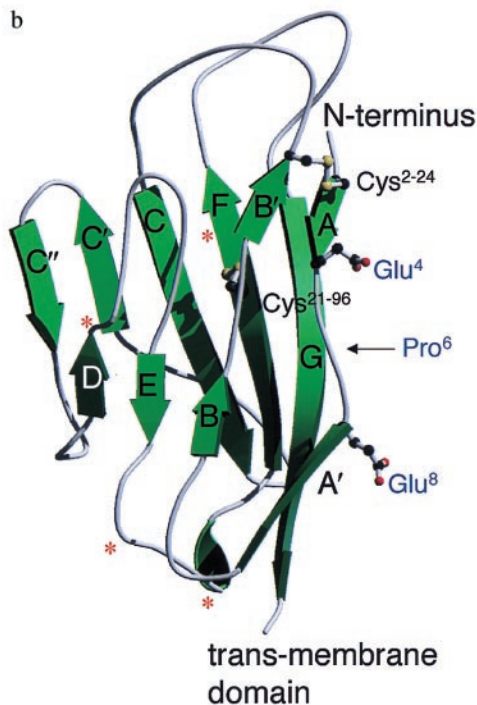
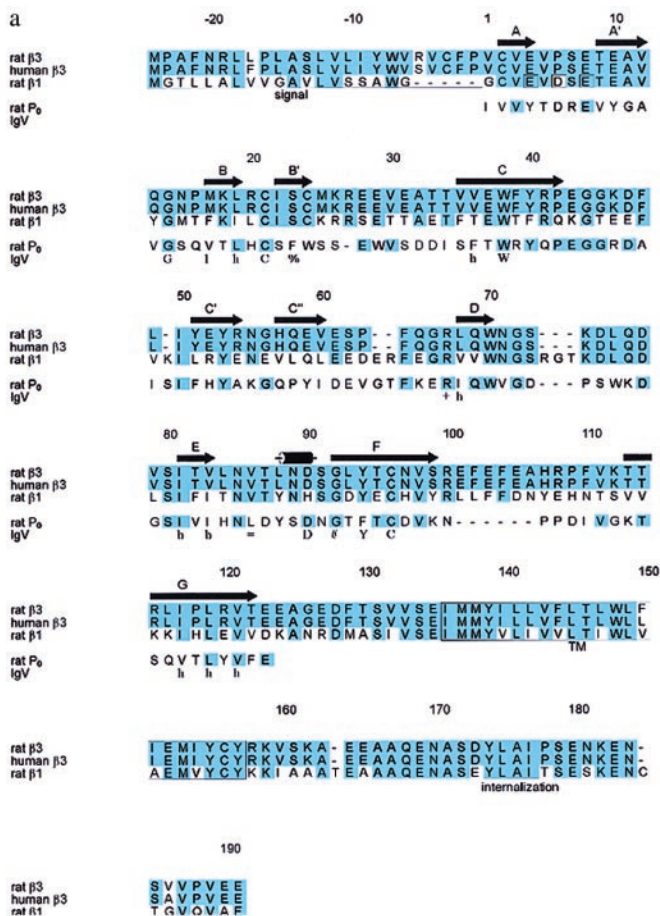


Fig. 3. Sequence comparison and three-dimensional modeling of β_3 . (a) Amino acid sequences of rat and human β_3 , aligned with the sequences of rat β_1 (SWISS-PROT Q00954; ref. 8) and the extracellular domain of rat myelin P₀ (SWISS-PROT P06907; ref. 29). The sequence numbering is based on rat β_3 , starting from the predicted N terminus of the mature protein. Amino acid identities with rat β_3 are indicated by shading. The putative signal sequence

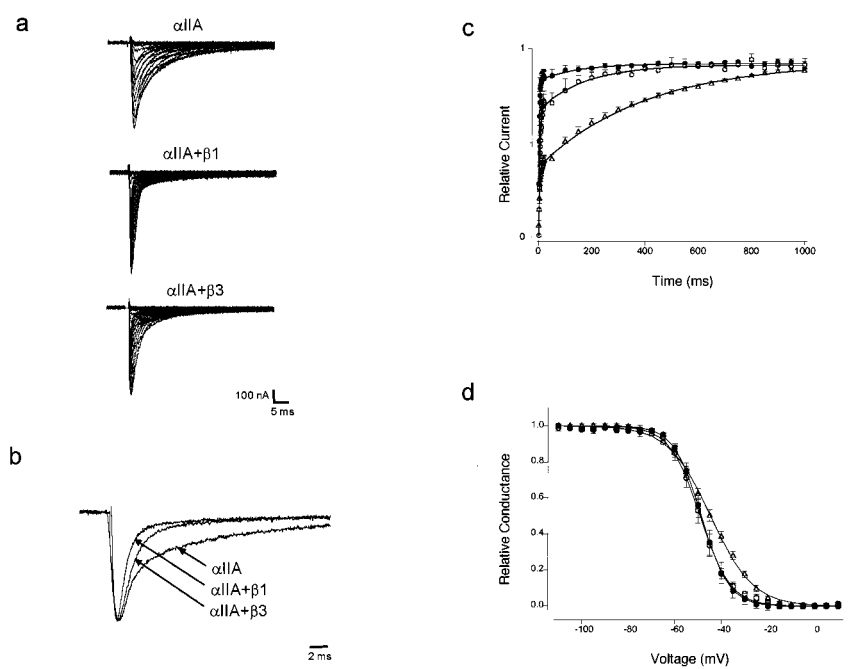
(Fig. 1b). With 0.5 ng of cDNA, abundant expression of both β_1 and β_3 was detected in adult rat brain with low but detectable β_3 expression in adrenal gland (from which the PC12 line originates) and kidney. Expression in other tissues was detectable only at the highest level of cDNA used (5 ng). As expected, abundant β_3 amplification product was apparent when cDNA derived from the parent PC12 cell line was used, but relatively little was apparent in the A35C variant.

The comparative distribution of β_3 - and β_1 -subunits within the adult rat central nervous system was investigated by *in situ* hybridization (Fig. 2) and is summarized in Table 1. A high level of β_3 mRNA was detected in many areas and had a largely complementary expression to that of β_1 mRNA. Thus, a high level of β_3 mRNA was present within forebrain structures such as the olfactory cortex and basal ganglia where a low level of β_1 mRNA was detected. In contrast, the level of β_3 mRNA expression was lower in thalamic nuclei but absent in the cerebellum where a high level of β_1 mRNA was evident. The complementary nature of β_1 and β_3 mRNA expression was even noticeable in individual layers of the neocortex where one of the two subunits was expressed at a higher level than the other (Table 1). The hippocampal formation was a striking exception, where both β_1 and β_3 were expressed at high levels. In general, α IIA-subunit mRNA was more comprehensively distributed, overlapping with both β_1 - and β_3 -subunit mRNAs. In certain areas, particularly the cerebellum, the distributions of α IIA and β_1 mRNA were remarkably similar, whereas in others, such as the basal ganglia and olfactory cortex, the α IIA message closely matched β_3 expression (Table 1).

Sequence of β_3 and Functional Inferences. The N-terminal 24 amino acids of the predicted β_3 protein sequence include a hydrophobic region preceded by a positive residue—typical features of a signal sequence (14). The location of the probable cleavage site (labeled 1 in Fig. 3a) is suggested by comparison with the experimentally confirmed site in β_1 (8) and supported by the presence of cysteine at position -3 (14). A hydrophobic region with strong α -helical propensity (residues 136–157) has the properties of a transmembrane domain and is conserved in β_1 (Fig. 3a). Thus, β_3 probably forms an extracellular N-terminal domain with a single membrane-spanning sequence and a C-terminal cytoplasmic region. Sodium channels undergo endocytosis from the plasma membrane (15). Interestingly, the putative cytoplasmic region of both β_3 and β_1 contains the sequence YLAI 16 amino acids from the end of the predicted transmembrane sequence. The position and sequence of this motif fits the consensus for an internalization signal recognized by clathrin-coated pits (16), suggesting a possible role for this class

and internalization signal are underlined and labeled. The putative transmembrane domain (TM) is boxed. Three negatively charged amino acid residues, previously identified as part of the α -subunit binding site of β_1 , are boxed. Invariant residues and the position of amino acids characteristic of the IgV domain are indicated beneath the sequence of myelin P₀: h, hydrophobic; l, aliphatic; #, neutral or hydrophobic; +, base; =, hydrophobic or Ser or Thr; #, Gly or Ala (rarely Asp; ref. 17). Secondary structure elements in the crystal structure of myelin P₀ (19) used to model β_3 are also shown: arrow, β -strand; cylinder, α - or 3_{10} -helix. The multiple alignment was generated with CLUSTALW (30) and formatted with ALSCRIPT (31). (b) The model for the three-dimensional structure of the mature extracellular domain (residues 1–123) of rat β_3 . The model was generated with MODELLER (32) by using the crystal structure of rat myelin P₀ (PDB 1neu; ref. 19) as a template and the alignment shown in a. The side chains of acidic residues in the putative α -subunit binding site are shown in ball-and-stick representation. Two predicted disulfide bonds are labeled in black. N-linked glycosylation sites (NXT and NXS; ref. 33) are indicated by asterisks. The potential glycosylation site on the F strand (N97) points away from the viewer and is below the plane of the paper. Fig. 3a was drawn with MOLSCRIPT (34) and RASTER3D (35). Note that in this model the B strand is broken into two parts labeled B and B', respectively. This secondary structure assignment is based on the definition of Kabsch and Sander (36) for the PDB entry 1neu and is different from the assignment described in the original paper (19).

Fig. 4. Coexpression of rat α IIA with rat β 3-subunit modifies inactivation kinetics. (a) Na^+ currents recorded from oocytes expressing rat α IIA, rat α IIA + rat β 1, and rat α IIA + rat β 3-subunits. Inward Na^+ currents were evoked by applying depolarizing pulses in 5-mV increments from a holding potential of -100 mV, from -80 mV to $+30$ mV. Duration of the pulses was 50 ms. (b) Normalized Na^+ currents from oocytes expressing rat α IIA, rat α IIA + rat β 1, and rat α IIA + rat β 3-subunits. Currents evoked by a voltage pulse to -10 mV were normalized to peak amplitudes. Inactivation of Na^+ currents at -10 mV were fitted with a double exponential decay: $I = A1 \exp(-t/\tau1) + A2 \exp(-t/\tau2) + C$, where A1 and A2 are the relative amplitudes of fast and slow components, $\tau1$ and $\tau2$ are the inactivation time constants, and C is the steady-state asymptote. See Table 2 for fit parameters. (c) Recovery from inactivation of α IIA coexpressed with β 1 or β 3. The recovery pulse protocol was a 1-s inactivating pulse to -10 mV followed by conditioning pulses to -100 mV for increasing periods of time (from 1–1,000 ms), followed by a test pulse to -10 mV. Points were sampled every 1 ms from 1 to 20 ms and then every 50 ms from 50 to 1,000 ms. Peak current amplitudes measured during the test pulse were normalized to the peak currents evoked during the inactivating pulse and were plotted as function of conditioning pulse duration. Δ , α IIA; \bullet , α IIA + β 1; \circ , α IIA + β 3. Data were fitted with a double exponential equation: $I = 1 - [A1 \exp(-t/\tau1) + A2 \exp(-t/\tau2)]$, where A1 and A2 are the relative amplitudes of recovery and $\tau1$ and $\tau2$ are the recovery time constants. See Table 2 for fit parameters. (d) Voltage-dependence of inactivation of α IIA coexpressed with β 1 or β 3. A two-step protocol was applied with a conditioning pulse of 500-ms duration from -110 mV to $+10$ mV in 5-mV increments, followed by a test pulse to -10 mV. Peak current amplitudes evoked by the test pulse were normalized to the maximum peak current amplitude and plotted as a function of the conditioning pulse potential. Δ , α IIA; \bullet , α IIA + β 1; \circ , α IIA + β 3. Data were fitted with a two-state Boltzman equation: $g = 1/[1 + \exp((V - V_{1/2})/k)]$, where g is conductance, $V_{1/2}$ is the voltage of half-maximal inactivation, and k is the slope factor. See Table 2 for fit parameters.



of β -subunit in the movement of sodium channels between cellular compartments.

As with β 1 and β 2, the extracellular domain of β 3 shows homology to proteins that adopt a V-type Ig fold (17, 18). Of these proteins, the extracellular domain of β 3 has the highest sequence identity to myelin P₀ (Fig. 3a). The known three-dimensional structure of myelin P₀ (19) was used as a template to model β 3 and thus identify regions of functional importance and facilitate a comparison with the previously predicted β 1 structure (20). The V-type Ig fold comprises 10 β -strands (labeled A, A', B, C, C', C'', D, E, F, and G) that form two antiparallel sheets packed face to face (17). The model predicts disulfide bonds at positions C21–96 and C2–24. The former is conserved in all V-type Ig domains and is likely to be structurally important, because its disruption in β 1 causes an inherited epilepsy syndrome (3). The latter is an unusual feature in Ig domains but its probable conservation in β 1 suggests a functional importance (Fig. 3a and b). It could for example help stabilize the A strand—a region implicated in α -subunit binding

(see below). Four N-linked glycosylation sites suggest a significant potential for posttranslational modification (Fig. 3a and b).

In both β 1 and β 3, the first 15 N-terminal residues of the mature protein form a predicted edge of β -pleated sheet. In β 1, an aspartic acid residue (D6) separates strands A and A'. This aspartic acid is flanked on either side by glutamic acid residues E 4 and E 8 (Fig. 3a). It has been shown that the simultaneous replacement of these acidic residues with neutral amino acids formed a protein that was less effective at promoting the fast gating mode of the channel (20). In β 3, the entire A/A' face is conserved with one exception: residue D6 of β 1 is replaced with a proline in β 3 (Fig. 3a and b). Proline tends to break β -strands, such that the gross conformation of the region should be conserved but with less pronounced negative potential. This difference is intriguing and suggested that β 3 might favor the fast gating mode less effectively than β 1 and thereby inactivate α -subunit opening more slowly.

Gating Kinetics of β 3. The rat sodium channel α IIA-subunit was expressed in *Xenopus* oocytes either alone or together with each

Table 2. Inactivation and recovery kinetic parameters

Subunit	Inactivation timecourse*				Recovery from inactivation*				Voltage-dependence of inactivation†		
	τ 1, ms	τ 2, ms	Percentage in fast mode	n	τ 1, ms	τ 2, ms	Percentage in fast mode	n	$V_{1/2}$, mV	k, mV	n
α IIA	2.4 ± 0.3	10.9 ± 1.3	46 ± 4	8	3.9 ± 0.2	446 ± 9	38 ± 0.4	5	-45.1 ± 0.3	9.8 ± 0.2	4
α IIA + β 1	1.4 ± 0.2	24.7 ± 4.3	95 ± 1	5	2.0 ± 0.1	148 ± 19	84 ± 0.4	5	-49.1 ± 0.3	5.9 ± 0.2	4
α IIA + β 3	1.5 ± 0.2	24.7 ± 4.3	85 ± 1	6	4.1 ± 0.2	170 ± 17	73 ± 1.2	5	-49.3 ± 0.2	6.1 ± 0.1	4

Analysis of inactivation and recovery kinetics of rat α IIA separately coexpressed with β 1- and β 3-subunits. The inactivation and recovery from inactivation time constants for different combinations of rat α IIA, rat β 1, and rat β 3 subunits are shown above separately calculated from data shown in Fig 4. Percentage in fast mode is the proportion of current described by the fast exponential time constant. This percentage is calculated by the equation $A1/(A1 + A2)$, where A1 and A2 are the amplitudes of the fast and slow exponential components, respectively. $V_{1/2}$ is the voltage of half-maximal inactivation, and k is the slope factor.

*There was a significant difference between the proportion of channels described by the fast gating mode for α IIA expressed alone compared to α IIA coexpressed with either β 1 or β 3 ($P < 0.001$) and between α IIA coexpressed with β 1 compared to β 3 ($P < 0.001$) as determined by Student's t test.

†There was a significant difference in $V_{1/2}$ and k for α IIA alone compared to α IIA expressed with either β 1 or β 3 ($P < 0.005$) as determined by Student's t test. Differences between $V_{1/2}$ and k for α IIA coexpressed with β 1 compared to β 3 were not statistically significant.

rat β -subunit, and the electrophysiological properties were compared (Fig. 4 and Table 2). In separate experiments, oocytes were injected with 0.2–1 ng of α IIA cRNA and 10 ng of β 1 or β 3 cRNA. These amounts are equivalent to a molar ratio of α IIA to β 1 or β 3 of between 1:50 and 1:400. When the cRNA molar ratio of α IIA to β 1 and β 3 was increased from 1:50 to 1:250, no significant change in inactivation kinetics was observed ($n = 7$ and $n = 9$, respectively), suggesting that the concentration of β -subunits was already saturating even at the lowest ratio used.

Oocytes expressing α IIA-subunits alone showed that inactivation at -10 mV was best fitted to a double exponential function, with time constants τ_1 and τ_2 corresponding to fast and slow gating modes, respectively (ref. 21; Fig. 4*a* and *b* and Table 2). There was no significant difference in the rates of inactivation or the proportion of current represented by each mode between different batches of oocytes (data not shown). Coexpression with β 1 or β 3 significantly increased the rate of current decay and the proportion of the total current described by τ_1 compared with α IIA expressed alone (Table 2). Most importantly, a greater proportion of current was described by the fast time constant for β 1 than for β 3. This result was highly significant ($P < 0.001$). Similar results were obtained when the fraction of channels in the fast gating mode was calculated by using recovery from inactivation data (Fig. 4*c* and Table 2). Both β 1 and β 3 altered the voltage-dependence of inactivation by the same amount, causing a hyperpolarizing shift in $V_{1/2}$ and a reduction in slope factor (Fig. 4*d* and Table 2). There was no change in peak current amplitude when α IIA was coinjected with β 1 or β 3 (range 0.1–8 μ A; $n = 6$ –9; three batches of oocytes).

Discussion

The discovery of the β 3-subunit is surprising insofar as the voltage-sensitive sodium channel is one of the best characterized of all the ion channels. Nevertheless, this discovery may help resolve a number of otherwise puzzling observations. For example, the specific labeling of sodium channels from fetal rat neurons identified a protein with β 1-like electrophoretic mobility, despite the near absence of β 1 mRNA from these cells (15).

Despite its importance in sodium channel function, the expression of β 1 can be regulated independently of α -subunits, as seen for example in the time course of its expression in fetal brain (22) and in the olfactory system after denervation (23). These results may be difficult to explain if β 1 is the only subunit of its type. Furthermore, it is surprising that the loss of function mutation in β 1 causing febrile seizure and generalized epilepsy (3) is not lethal considering that such a mutation would be expected to compromise sodium channel kinetics globally. It is possible that β 3 may act in a compensatory manner, and it will be interesting to see whether β 3 expression is enhanced in this situation.

The human β 3 gene has been mapped to chromosome 11q23.3. Interestingly, the gene for β 2 and the human N-CAM gene, which contains a V-type Ig domain, are also localized close to this region (24, 25). These distantly related genes most likely

evolved by repeated duplication, and it will be interesting to examine the region in detail for other β -homologues. In contrast, the β 1 gene is localized on chromosome 19 (3).

Within the central nervous system, some neurons express low levels of β 1 (26, 27). Our results show that in most of these areas there is a correspondingly high level of β 3 expression and considerable overlap of α IIA expression in areas covered by both β 1- and β 3-subunits. Hence, both subunits may be natural partners for α IIA in different regions of the brain. It is known that β 1 can bind a range of α -subunits (22). Given the high level of conservation in the A/A' face of the molecule, a similar degree of flexibility is to be expected in β 3. A quantitative analysis with subunit-specific antibodies and a comprehensive study of α - and β -isoform expression in different brain regions should help address this question.

Both β 1 and β 3 cause a hyperpolarizing shift in the voltage-dependence of inactivation and modulate the α -subunit by increasing the fraction of channels operating in the fast gating mode. Together with the sequence homology, this result suggests that β 1 and β 3 are structurally distinct members of a single functional class of auxiliary subunits. Nevertheless, there are also clear differences in the detailed kinetic effects of β 3. Significantly more channels operated in the fast gating mode in the presence of β 1-subunit compared with β 3. From the structural model and known properties of β 1, we suggest that the substitution of a proline for an aspartic acid at residue 6 may play a role in this difference. Clearly, it will be important to confirm this proposal by site-directed mutagenesis. Previous work has reported a 2.5-fold increase in current amplitude in the presence of β 1, implying an enhanced expression of channel subunits at the plasma membrane (8). In our experiments, the coexpression of either β 1- or β 3- with the α IIA-subunit did not increase the peak current amplitude. Recent studies also show that β 1 has no effect on peak current amplitude when coexpressed with α II or α IIA in *Xenopus* oocytes (28). The reason for this difference is not clear, but channel expression will depend on several factors such as translation efficiency of microinjected cRNA and the saturation of the constitutive secretory pathway in the injected oocytes, and these factors may complicate the interpretation of peak current data.

The discovery of another β -subunit is important in that it confers a further layer of complexity to sodium channels, reveals additional opportunities to make subtle changes to sodium channel gating, and thereby allows the nervous system extra capacity to process and respond to diverse information.

We thank Prof. W. A. Catterall (Department of Pharmacology, University of Washington) and Dr. L. L. Isom (Department of Pharmacology, University of Michigan) for cDNA clones encoding the rat sodium channel α IIA- and β 1-subunits. This work was supported by a project grant to A.P.J. from the Wellcome Trust and a grant to P.J.R. from the Parke–Davis Neuroscience Research Centre. K.M. thanks the Human Frontier Science Program for financial support.

- Marban, E., Yamagishi, T. & Tomaselli, G. F. (1998) *J. Physiol.* **508**, 647–657.
- Hartshorne, R. P. & Catterall, W. A. (1984) *J. Biol. Chem.* **259**, 1667–1675.
- Wallace, R. H., Wang, D. W., Singh, R., Scheffer, I. E., George, A. L., Jr., Phillips, H. A., Saar, K., Reis, A., Johnson, E. W., Sutherland, G. R., et al. (1998) *Nat. Genet.* **19**, 366–370.
- Cannon, S. (1996) *Annu. Rev. Neurosci.* **19**, 141–164.
- Wang, Q., Shen, J., Splawski, I., Atkinson, D., Li, Z., Robinson, J. L., Moss, A. J., Towbin, J. A. & Keating, M. T. (1995) *Cell* **80**, 805–811.
- Taylor, C. P. & Meldrum, B. S. (1995) *Trends Pharmacol. Sci.* **16**, 309–316.
- Isom, L. L., De Jongh, K. & Catterall, W. A. (1994) *Neuron* **12**, 1183–1194.
- Isom, L. L., De Jongh, K., Patton, D., Reber, B., Offord, J., Charbonneau, H., Walsh, K., Goldin, A. L. & Catterall, W. (1992) *Science* **256**, 839–842.
- Isom, L. L., Ragsdale, D., De Jongh, K., Westenbroek, R., Reber, B., Scheuer, T. & Catterall, W. (1995) *Cell* **83**, 433–442.
- Pance, A., Morgan, K., Guest, P. C., Bowers, K., Dean, G. E., Cutler, D. F. & Jackson, A. P. (1999) *J. Neurochem.* **73**, 21–30.
- Ausubel, F., Kingston, R., Moore, D., Seidman, J., Smith, J. & Struhl, K., eds. (1988) *Current Protocols in Molecular Biology* (Wiley, New York).
- Diatchenko, L., Lau, Y. F., Campbell, A. P., Chenchik, A., Moqadam, F., Huang, B., Lukyanov, S., Lukyanov, K., Gurskaya, N., Sverdlov, E. D., et al. (1996) *Proc. Natl. Acad. Sci. USA* **93**, 6025–6030.
- Gyapay, G., Schmitt, K., Fizames, C., Jones, H., Vega-Czarny, N., Spillet, D., Musclet, D., Prud'Homme, J. F., Dib, C., Auffray, C., et al. (1996) *Hum. Mol. Genet.* **5**, 339–346.
- Von Heijne, G. (1983) *Eur. J. Biochem.* **133**, 17–21.
- Paillart, C., Boudier, J. L., Boudier, J. A., Rochat, H., Couraud, F. & Dargent, B. (1996) *J. Cell Biol.* **134**, 499–509.
- Marks, M. S., Ohno, H., Kirchhausen, T. & Bonifacio, J. S. (1997) *Trends Cell Biol.* **7**, 124–128.
- Harpaz, Y. & Chothia, C. (1994) *J. Mol. Biol.* **238**, 528–539.
- Isom, L. L. & Catterall, W. A. (1996) *Nature (London)* **383**, 307–308.
- Shapiro, L., Doyle, J. P., Hensley, P., Colman, D. R. & Hendrickson, W. A. (1996) *Neuron* **17**, 435–449.
- McCormick, K. A., Isom, L. L., Ragsdale, D., Smith, D., Scheuer, T. & Catterall, W. A. (1998) *J. Biol. Chem.* **273**, 3954–3962.
- Hebert, T. E., Monette, R., Dunn, R. J. & Drapeau, P. (1994) *Proc. R. Soc. London Ser. B.* **256**, 253–261.
- Patton, D. E., Isom, L. L., Catterall, W. A. & Goldin, A. L. (1994) *J. Biol. Chem.* **269**, 17649–17655.
- Sashihara, S., Greer, C. A., Oh, Y. & Waxman, S. G. (1996) *J. Neurosci.* **16**, 702–713.
- Eubanks, J., Srinivasan, J., Dinulos, M. B., Distèche, C. M. & Catterall, W. A. (1997) *NeuroReport* **8**, 2775–2779.
- Nguyen, C., Mattei, M.-G., Mattei, J.-F., Santoni, M.-J., Goridis, C. & Jordan, B. R. (1986) *J. Cell. Biol.* **102**, 711–715.
- Sashihara, S., Oh, Y., Black, J. A. & Waxman, S. G. (1995) *Brain Res. Mol. Brain Res.* **34**, 239–250.
- Oh, Y., Sashihara, S. & Waxman, S. G. (1994) *Neurosci. Lett.* **176**, 119–122.
- Toib, A., Lyakhov, V. & Marom, S. (1998) *J. Neurosci.* **18**, 1893–1903.
- Lemke, G. & Axel, R. (1985) *Cell* **40**, 501–508.
- Higgins, D. G., Thompson, J. D. & Gibson, T. J. (1996) *Methods Enzymol.* **266**, 383–402.
- Barton, G. J. (1993) *Protein Eng.* **6**, 37–40.
- Sali, A. & Blundell, T. L. (1993) *J. Mol. Biol.* **234**, 779–815.
- Kornfeld, R. & Kornfeld, S. (1985) *Annu. Rev. Biochem.* **54**, 631–664.
- Kraulis, P. J. (1991) *J. Appl. Crystallogr.* **24**, 946–950.
- Merrit, E. & Murphy, M. (1994) *Acta Crystallogr. D* **50**, 869–873.
- Kabsch, W. & Sander, C. (1983) *Biopolymers* **22**, 2577–2637.